Search for Doubly Radiative *np* Capture*

R. G. Arnold and B. T. Chertok
The American University, Washington, D. C. 20016

I. G. Schröder
National Bureau of Standards, Washington, D. C. 20234

J. L. Alberi
Harvard University, Cambridge, Massachusetts 02138

(Received 17 May 1973)

We have made a search for doubly radiative *np* capture $n+p \rightarrow \gamma_1+\gamma_2+{}^2\mathrm{H}$. It has been suggested that this process might contribute to the total *np*-capture cross section and thus explain the long-standing discrepancy in *np* capture ($\sigma_{\mathrm{expt}}=334.2\pm0.5$ mb and $\sigma_{\mathrm{th}}=302.5\pm4.0$ mb). Previous *np*-capture experiments have been insensitive to the energy distribution of the capture γ rays. In this experiment we searched for two-photon events by looking for γ rays in coincidence from a H_2O target exposed to a beam of thermal neutrons using two 5×5-cm NaI detectors. Analysis of the coincidence spectra indicates two-photon *np*-capture events have not been observed. An upper limit at the 3 standard deviation confidence level of $\sigma_{2\gamma} \leq 1.0$ mb can be placed on the doubly radiative *np*-capture cross section. Therefore the two-photon cross section does not explain the discrepancy between the theoretical and experimental *np*-capture cross sections.

I. INTRODUCTION

The *np* radiative capture process $n+p \rightarrow 2\gamma+{}^2\mathrm{H}$ is understood at the 9% level, that is

$$\frac{\sigma_{\mathrm{expt}}-\sigma_{\mathrm{th}}}{\sigma_{\mathrm{expt}}}=9.5\%. \tag{1.1}$$

This discrepancy, which represents about 30 mb at thermal-neutron energies, has been the subject of many theoretical investigations with conflicting claims of success and failure over the years.[1] While the measured cross section has stabilized at $\sigma_{\mathrm{expt}}=334.2\pm0.5$ mb,[2] the theoretical value has fluctuated about the value of 302.5 ±4.0 mb[3] from effective-range theory. Following a suggestion of Adler, Chertok and Miller[1] that some or all of this discrepancy could be due to doubly radiative capture

$$n+p \rightarrow \gamma_1+\gamma_2+{}^2\mathrm{H}, \tag{1.2}$$

we have undertaken a search for this decay mode. The results of that search are the subject of this report.

Since this measurement was completed, several new calculations and speculations have appeared.[4-10] Two of these new calculations[8,10] include the catastrophic pion current, which had been omitted in earlier works, and a rescattering current which is in qualitative agreement with the 3-3 resonance contribution previously calculated by Stranahan.[11] Agreement with experiment is reported[8,10] although the question of double counting of resonance and pion currents carried over from high-energy duality leaves the good quantitative agreement in some doubt.[10] A more complete treatment of the negative-energy parts of the catastrophic pion current is a further question. This is being examined with two-nucleon negative-energy wave functions.[12]

Of particular relevance to our work is Adler's calculation[5] of the two-photon-capture cross section. He treats this process by a Compton-nucleon amplitude for two-γ emission constrained by the isotopics of the two-nucleon system. The resulting amplitude reduces properly in the low-energy limit to the classical result of Goldberger, Gell-Mann, and Low.[13] The predicted cross section is very small because of almost complete cancellation of individual amplitudes. From the ${}^1S_0$ *np*-capture state

$$\sigma_{2\gamma}/\sigma_{\gamma}=3.4\times10^{-10} \tag{1.3}$$

and from the ${}^3S_1$ *np*-capture state

$$\sigma_{2\gamma}/\sigma_{\gamma}=4.8\times10^{-13} \tag{1.4}$$

Adler examines the speculation of Breit and Rustgi[6] that the ${}^3S_1$ continuum *np* and the ${}^3S_1$ deuteron wave functions are not completely orthogonal. Using Eq. (1.1) as a measure of this nonorthogonality, he calculates a very large enhancement to Eq. (1.4) ${}^3S_1 \rightarrow {}^3S_1+2\gamma$,

$$\sigma_{2\gamma}/\sigma_{\gamma}=1.4\times10^{-4} \tag{1.5}$$

or $\sigma_{2\gamma}=42\ \mu$b. Unfortunately, the present experiment is not sensitive to such a small cross section, but it does test the two-photon hypothesis

in the region

$$\sigma_{2\gamma}/\sigma_{\gamma} = 2 \text{ to } 3\times10^{-3}. \quad (1.6)$$

II. EXPERIMENTAL METHOD

The method used in this experiment to search for two-photon np capture was to look for γ rays of the appropriate energy emerging in coincidence from a water target exposed to a beam of thermal neutrons as in Fig. 1. The spectrum of γ rays from two-photon events is continuous with

$$E_1 + E_2 = 2.2 \text{ MeV} \quad (2.1)$$

and is expected to be peaked at $E_1 = E_2$.[5] The phase space of the two-photon events is schematically represented in Fig. 2(a). The experimental strategy is determined primarily by the requirement of detecting γ rays with a broad energy distribution that are in true coincidence amidst a large background of accidental coincidences and unwanted prompt coincidences from other neutron-induced reactions in the target. The cross section for doubly radiative capture is determined here relative to the cross section for single-photon capture by comparing the signal-coincidence counting rate with the singles counting rate for 2.2-MeV capture γ rays from the same target.

The signal-coincidence counting rate can be expressed as

$$R_{2\gamma} = \phi N_p \sigma_{2\gamma} \epsilon_1(E_1)\epsilon_2(E_2) f, \quad (2.2)$$

where ϕ is the incident neutron flux, N_p is the number of protons exposed to the neutron beam, and $\sigma_{2\gamma}$ is the cross section for np capture leading to two-photon emission. The symbols $\epsilon_1(E_1)$ and $\epsilon_2(E_2)$ represent the efficiencies for detection of a photon of energy E_1 MeV in detector 1 and a photon of energy $E_2 = 2.2 - E_1$ MeV in detector 2.

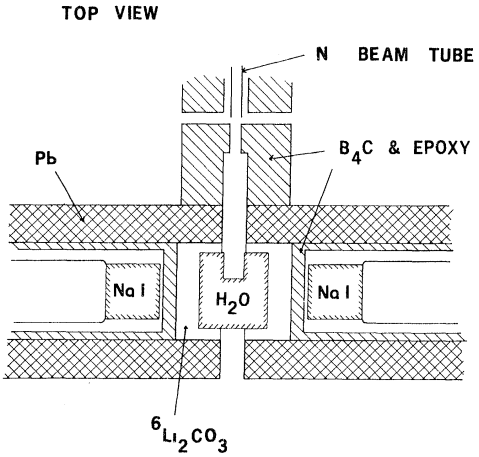

FIG. 1. np-capture geometry.

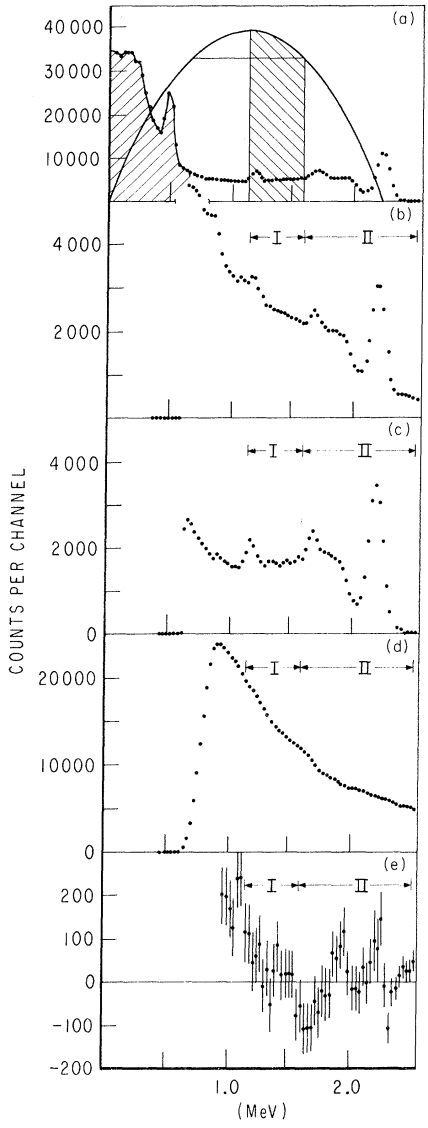

FIG. 2. (a) The two-photon phase space and a singles spectrum with the H_2O target. The spectrum from one detector is plotted to indicate the response of the NaI detector to the large flux of 2.2-MeV γ rays from single-photon np capture. The phase space of the two-photon events is schematically indicated by the curve peaked at 1.1 MeV. The shaded region below 0.6 MeV was biased out in both legs during the coincidence runs. The region marked I from 1.1 to 1.6 MeV represents the useful signal region. Region II was used for normalization in the background subtraction. (b) The prompt-coincidence spectrum F with the H_2O target. (c) The delayed-coincidence spectrum D with the H_2O target. (d) The prompt-coincidence spectrum B with the D_2O target. (e) The residual spectrum $R_i = F_i - C_1 D_i - C_2 B_i$ with normalization constants C_1 and C_2 determined by minimizing the residuals in region II.

The factor f represents that fraction of phase space of the two-photon events in the range of energies accepted by the detection system.

The singles counting rate for the 2.2-MeV γ rays is given by

$$R_\gamma = \phi N_p \sigma_\gamma \epsilon_1(2.2). \tag{2.3}$$

Here σ_γ is the cross section for single-photon np capture and $\epsilon_1(2.2)$ is the efficiency for detection of 2.2-MeV capture γ rays in detector 1. Taking the ratio of Eqs. (2.2) and (2.3) gives

$$\sigma_{2\gamma} = \sigma_\gamma \frac{R_{2\gamma}}{R_\gamma} \frac{\epsilon_1(2.2)}{\epsilon_1(E_1)\epsilon_2(E_2) f}. \tag{2.4}$$

The quantities ϕN_p divide out of the ratio because the singles and coincidence measurements are made with the same target and neutron beam.

III. APPARATUS

A beam of filtered (MgO) thermal neutrons[14] was extracted from the National Bureau of Standards reactor, transported through a 5-m-long 1.27-cm-diam Ni-coated totally reflecting glass tube, and passed into the target located between two 5×5-cm NaI detectors. The geometry of the beam tube, target, and detectors is illustrated in Fig. 1. The target material was 175 g of H_2O in a lucite cylinder 6 cm in diameter and 7 cm long with 0.16-cm wall thickness. Lucite has a composition $(C_5H_8O_2)_x$. Background spectra were also obtained with D_2O in place of the H_2O. The beam tube and detectors were surrounded with layers of B_4C in epoxy to absorb stray neutrons by the reaction $^{10}B(n, \alpha)^7Li$ ($\sigma = 3840$ b). The H_2O target was surrounded with a layer of isotopically enriched (95.54 at.%) $^6Li_2CO_3$ in a Lucite container to absorb neutrons via the reaction $^6Li(n, \alpha)^3H$ ($\sigma = 950$ b). ^6Li was preferred as it produces 10^5 less γ rays than the $^{10}B(n, \alpha)^7Li$ reaction. In the latter reaction 96% of all α particles lead to a 0.477-MeV excited state of ^7Li producing copious γ rays of this energy which when located near the detectors causes excessive accidental coincidence rates. The coincidence electronics were arranged in a "fast-slow" configuration and is shown in Fig. 3. RCA 8575 photomultiplier tubes were used for fast timing and good energy resolution. With a ^{60}Co source the peak in the start-minus-stop spectrum from the time-to-amplitude converter had a full width at half maximum of 1.8 nsec. A single channel was set centered on this peak and 6 nsec wide. The energy resolution of the system was 5% at 1.3 MeV.

IV. EXPERIMENTAL PROCEDURE

The main difficulty in this experiment is caused by the large background generated by γ rays from the target and materials surrounding the target.

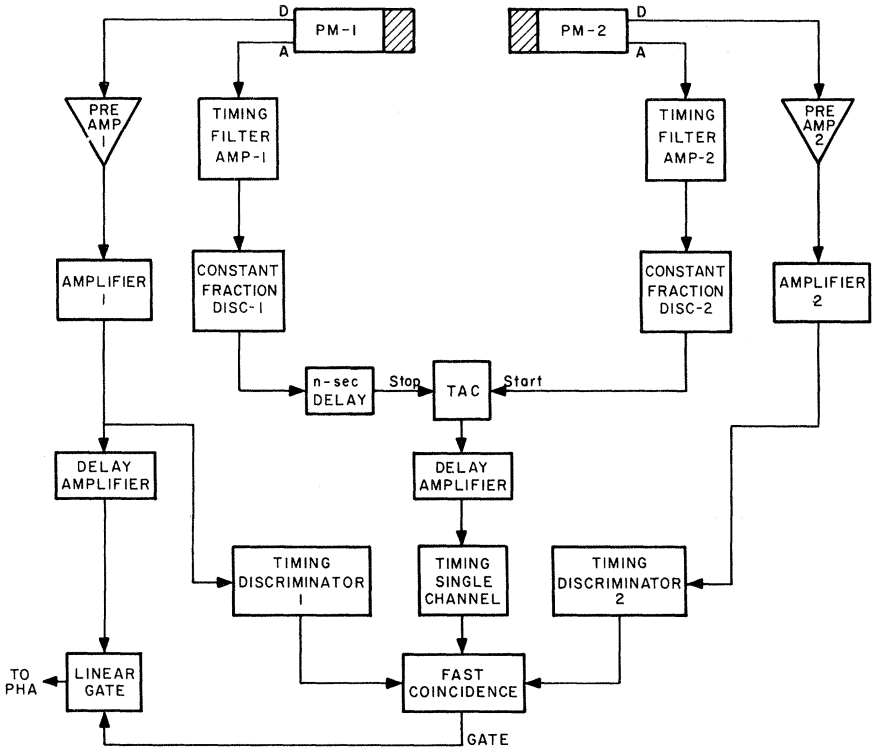

FIG. 3. Block diagram of the electronics.

The geometry of Fig. 1 is the result of the compromise between the conflicting requirements for shielding the detectors from the scattered neutrons and the desire for large solid angles and small amounts of nonhydrogenous materials near the neutron beam. The primary source of unwanted coincidences is the accidentals caused by pulses from unrelated photons arriving at the coincidence gate within the 6-ns resolving time, primarily from 2.2-MeV γ rays from single-photon-capture events. To help reduce the accidental rate the portion of the spectrum below 0.6 MeV was biased out in each leg. Thus the large number of pulses arising from 0.511-MeV anihilation radiation [See Fig. 2(a)] were rejected, with a 44% loss of signal phase space. To obtain sufficient information to deduce the two-photon coincidence rate three kinds of spectra were obtained. Foreground plus background, herein labeled F and illustrated in Fig. 2(b), were accumulated in straightforward coincidence runs with the H_2O target in place. The accidental component was measured in delayed-coincidence spectra, here labeled D and illustrated in Fig. 2(c), obtained with an arbitrary delay in one leg of the coincidence circuit using the H_2O target. The background-prompt-coincidence spectrum from γ-ray cascades following neutron capture, primarily in ^{16}O ($\sigma = 0.18$ mb) and ^{12}C ($\sigma = 3.4$ mb) in and near the H_2O target, cannot be measured directly. A close approximation to this background spectrum was determined here by recording the prompt coincidences with D_2O substituted for H_2O in the target chamber. These spectra are labeled B and displayed in Fig. 2(d). The object of these measurements was to duplicate the coincidence background from γ-ray cascades in ^{17}O, ^{13}C, and other nuclei under conditions as nearly like those for the H_2O target as possible, but without the large accidental counting rate from np-capture γ rays. The deuterium-capture cross section is 0.5 mb or about 1/700 of the np-capture cross section.

The data taking was broken into a series of separate runs with counting times ranging from 2×10^3 to 4×10^3 min. The energy calibration was determined from the first- and second-escape peaks in the singles spectra taken with each detector before or after each run. Slight gain and baseline shifts were accounted for in the analysis.

V. REDUCTION OF DATA

The analysis is divided into two parts. The first step is to extract the signal-coincidence counting rate from the signal-plus-background spectrum F. Then the cross section $\sigma_{2\gamma}$ is determined by comparison with the known cross section σ_γ for single-photon capture by comparing the coincidence counting rate with the singles counting rate at 2.2 MeV, after suitable corrections are made for absorptions, detector efficiencies and solid angles, and the fraction of phase space available. For purposes of analysis the spectra have been divided into two regions (See Fig. 2). Region I is that portion of the spectrum expected to contain signal-coincidence counts. It is bounded on the upper side at 1.6 MeV because of the constraint of Eq. (2.1) and the bias on the gating detector which rejected all pulses corresponding to photopeak events up to 0.6 MeV. In principle, region I could be extended on the lower side down to 0.6 MeV where the bias was placed in detector 1, but it was extended only to 1.2 MeV. The lower half of the spectrum contains larger sources of systematic error due to larger numbers of background counts and slight drifts in the detector electronics during the long counting times. Region II extends from 1.6 MeV to the upper end of the spectrum. It does not contain any signal counts because of the bias and the constraint of Eq. (2.1). The procedure of extracting the coincidence signal is as follows. All the individual spectra of each type were adjusted to the same gain (30 keV/channel) and baseline and summed.[15] These summed spectra are displayed in Figs. 2(b)–2(d). The signal component in region I of spectrum F was extracted by subtracting out the background components D and B after suitable normalization. The normalization constants C_1 and C_2 were determined by requiring that the residuals

$$R_i = F_i - C_1 D_i - C_2 B_i , \tag{5.1}$$

where i ranges over the channels in region II, be a minimum in the least-squares sense.[16] No attempt was made to determine the absolute normalization as this would have required accurate knowledge of the neutron flux.

The problem is reduced to finding C_1 and C_2 which give a minimum for the χ^2:

$$\chi^2 = \sum_i^{\mathrm{II}} (1/\sigma_i^{\,2})(F_i - C_1 D_i - C_2 B_i)^2 .$$

The sum is over the channels in region II. The variance $\sigma_i^{\,2}$ on the residual R_i in the i^{th} channel is given by

$$\sigma_i^{\,2} = \sigma_{F_i}^{\,2} + C_1^{\,2}\sigma_{D_i}^{\,2} + D_i^{\,2}\sigma_{C_1}^{\,2} + C_2^{\,2}\sigma_{B_i}^{\,2} + B_i^{\,2}\sigma_{C_2}^{\,2} + 2D_i B_i \sigma_{C_1 C_2} ,$$

where $\sigma_{F_i}^{\,2}$, $\sigma_{D_i}^{\,2}$, and $\sigma_{B_i}^{\,2}$ are the statistical errors on the spectra F_i, D_i, and B_i, and σ_{C_1} and σ_{C_2} are the variances and $\sigma_{C_1 C_2}$ is the covariance on the parameters C_1 and C_2. This expression for $\sigma_i^{\,2}$ follows by taking the square of the propogated error on the residual of Eq. (5.1) and dropping all cross terms containing independently measured

quantities.

The normalization constants which give χ^2 a minimum satisfy

$$\frac{\partial\chi^2}{\partial C_1}=0\,,\quad \frac{\partial\chi^2}{\partial C_2}=0\,. \tag{5.2}$$

The nonlinear Eqs. (5.2) cannot be solved directly for C_1 and C_2. The procedure adopted here was to linearize the equations and solve them iteratively. Initial values for C_1 and C_2 were used to evaluate σ_i^2. With these numerical values the linearized Eqs. (5.2) were solved for new values of C_1 and C_2 and the variance-covariance matrix determined.[16] The results were recycled into a new determination of σ_i^2 and the process repeated until the total residual in region II

$$N_{\rm II}=\sum_i^{\rm II}(F_i - C_1D_i - C_2B_i) \tag{5.3}$$

converged, usually in about three steps. The normalization constants thus determined were used to evaluate the difference of Eq. (5.3) in region I.

The variance on the difference $N_{\rm I}$ or $N_{\rm II}$ is given by

$$\sigma_N^2=\frac{\chi^2}{\nu}\left[\sigma_F^2+C_1^2\sigma_D^2+D^2\sigma_{C_1}^2+C_2^2\sigma_B^2 + B^2\sigma_{C_2}^2+2\,DB\sigma_{C_1C_2}\right],$$

where $D^2=(\Sigma D_i)^2$ and $B^2=(\Sigma B_i)^2$ and σ_F^2, σ_B^2 and σ_D^2 are the squares of the statistical errors on the sums over the regions I or II. The propagated error is augmented by the factor χ^2/ν, the χ^2 per degree of freedom. This increases the error to account for differences between our model, namely that the residuals are zero in region II, and the data, which when compared with that model yielded a normalized χ^2 larger than unity. The χ^2 is larger than unity because of small differences between the foreground and background spectra. We know for instance that the spatial distribution of neutrons is different in the H_2O than in D_2O because of different scattering and absorption cross sections. This could lead to differences in the shapes of the coincidence spectra caused by edge effects in the NaI detectors and by different numbers of neutrons being captured in the ^{16}O and ^{12}C in the target walls and Li_2CO_3. Other slight differences between the spectra can be expected due to small gain and baseline shifts during the runs.

The results of the normalization and subtraction are

$$N_{\rm I}=470\pm450 \text{ counts/4600 min},$$

$$N_{II}=80\pm525 \text{ counts/4600 min}.$$

These errors include enhancement by the normalized χ^2

$$\frac{\chi^2}{\nu}=1.74$$

with $\nu=29$ degrees of freedom. Figure 2(e) is a plot of the residual spectrum. The signal-coincidence counting rate is then

$$R_{2\gamma}=0.10\pm0.10 \text{ counts/min}.$$

The singles counting rate R_γ for the 2.2-MeV γ rays from *np* capture was extracted from the singles spectra, Fig. 2(a), by measuring the area under the 2.2-MeV photopeak. The value was

$$R_\gamma=65\,000\pm250 \text{ counts/min}.$$

The detector efficiencies in Eq. (2.4) were computed by numerically integrating over the target volume the product of the photopeak efficiency times electronic absorption weighted by the neutron distribution. The photopeak efficiencies were determined from values published by Vegors Marsden, and Heath.[17] The fraction f of phase space of the two-photon events covered by region I is 0.28.

VI. RESULTS AND CONCLUSIONS

The observed signal-coincidence counting rate of 0.10 ± 0.10 counts/min is consistent with nonobservation of doubly radiative *np* capture. Using a value of 0.20 counts/min, which is at the upper edge of the error bar, in Eq. (2.4) together with the theoretical one-γ *np* cross section $\sigma_\gamma=302$ mb[1] yields an upper limit for the cross section

$$\sigma_{2\gamma}\leq0.6 \text{ mb}.$$

A more conservative upper limit of 0.30 counts/min, which is 2 standard deviations from the observed value of 0.10 counts/min or nearly 3 standard deviations from the null, corresponds to an upper limit of

$$\sigma_{2\gamma}\leq0.8 \text{ mb}.$$

We conclude that two-photon *np*-capture events have not been observed and suggest an upper limit for the cross section of

$$\sigma_{2\gamma}\leq1.0 \text{ mb}.$$

Therefore any two-γ cross section cannot account for the 32-mb discrepancy between the measured *np* absorption cross section and the effective-range theory prediction.

ACKNOWLEDGMENTS

The authors wish to thank R. A. Dallatore for his able assistance during the course of the experiment as well as for constructing the target assemblies, and E. O. Edney for his help in setting up the totally reflecting neutron pipe. Helpful discussions with R. J. Adler and M. Danos on the two-photon problem are gratefully acknowledged.

*Research supported in part under National Science Foundation Grant No. 16565.

[1]R. J. Adler, B. T. Chertok, and H. C. Miller, Phys. Rev. C 2, 69 (1970). This paper contains a concise review of the np-capture problem and references to earlier work.

[2]A. Cox, S. Wynchank, and C. Collie, Nucl. Phys. 74, 481 (1965).

[3]H. P. Noyes, Nucl. Phys. 74, 508 (1965). This paper is a review of the numerous improvements to the zero-range approximation and it contains an extensive bibliography.

[4]R. J. Adler, Phys. Rev. C 5, 615 (1972).

[5]R. J. Adler, Phys. Rev. C 6, 1964 (1972).

[6]G. Breit and M. L. Rustgi, Nucl. Phys. A161, 337 (1971).

[7]S. S. Malik, Phys. Rev. C 5, 1807 (1972).

[8]D. O. Riska and G. E. Brown, Phys. Lett. 38B, 193 (1972).

[9]F. Kaschluhn and K. Lewin, Nucl. Phys. B49, 525 (1972).

[10]M. Gari and A. H. Huffman, Phys. Rev. C 7, 994 (1973).

[11]G. Stranahan, Phys. Rev. 135, B953 (1964).

[12]E. Dressler, R. J. Adler, and F. Gross, private communication; F. Gross, Phys. Rev. (to be published).

[13]M. Gell-Mann and M. Goldberger, Phys. Rev. 96, 1433 (1954); F. Low, *ibid* 96, 1428 (1954).

[14]S. Holmroyd and D. Conner, Rev. Sci. Instrum. 40, 49 (1969).

[15]The spectra were analyzed using a version of the program SAMPO developed by J. T. Routti and S. G. Prussin, Nucl. Instrum. Methods 72, 125 (1969), modified here to include facilities for shifting the gain and adding spectra.

[16]For a description of the methods of maximum likelihood see P. R. Bevington, *Data Reduction and Error Analysis for the Physical Sciences* (McGraw-Hill, New York, 1969).

[17]S. H. Vegors, Jr., L. L. Marsden, and R. L. Heath, AEC Report No. IDO-16370, 1958 (unpublished).